Journal of Power Sources 194 (2009) 456–466

Contents lists available at ScienceDirect

Journal of Power Sources

journal homepage: www.elsevier.com/locate/jpowsour

Decentralized generation of electricity from biomass with proton exchange membrane fuel cell

Richard Toonssen*, Nico Woudstra, Adrian H.M. Verkooijen

Delft University of Technology, Faculty of Mechanical, Marine and Material Engineering, Process and Energy Department, Section Energy Technology, Leeghwaterstraat 44, 2628 CA Delft, The Netherlands

ARTICLE INFO

Article history:
Received 16 March 2009
Received in revised form 7 May 2009
Accepted 25 May 2009
Available online 6 June 2009

Keywords:
Biomass gasification
PEM fuel cell
Exergy analysis
Decentralized power production

ABSTRACT

Biomass can be applied as the primary source for the production of hydrogen in the future. The biomass is converted in an atmospheric fluidized bed gasification process using steam as the gasifying agent. The producer gas needs further cleaning and processing before the hydrogen can be converted in a fuel cell; it is assumed that the gas cleaning processes are able to meet the requirements for a PEM-FC. The compressed hydrogen is supplied to a hydrogen grid and can be used in small-scale decentralized CHP units. In this study it is assumed that the CHP units are based on low temperature PEM fuel cells. For the evaluation of alternative technologies the whole chain of centralized hydrogen production from biomass up to and including decentralized electricity production in PEM fuel cells is considered.

Two models for the production of hydrogen from biomass and three models for the combined production of electricity and heat with PEM fuel cells are built using the computer program Cycle-Tempo. Two different levels of hydrogen purity are considered in this evaluation: 60% and 99.99% pure hydrogen. The purity of the hydrogen affects both the efficiencies of the hydrogen production as well as the PEM-FC systems. The electrical exergy efficiency of the PEM-FC system without additional heat production is calculated to be 27.66% in the case of 60% hydrogen and 29.06% in the case of 99.99% pure hydrogen. The electrical exergy efficiencies of the whole conversion chain appear to be 21.68% and 18.74%, respectively. The high losses during purification of the hydrogen gas result in a higher efficiency for the case with low purity hydrogen. The removal of the last impurities strongly increases the overall exergy losses of the conversion chain.

1. Introduction

Environmental concerns lead to the search for sustainable energy sources for the future and also more efficient ways to convert fuel into energy. One of the promising primary energy sources is biomass. Due to its short carbon dioxide cycle, biomass is considered carbon dioxide neutral. Most biomass sources are solid, like wood. These solid biomass sources are hard to handle [1], so they have to be converted into a more convenient secondary energy carrier to enable the conversion of these fuels in advanced conversion systems with gas turbines and/or fuel cells. By biomass gasification hydrogen rich can be produced, which mainly contains hydrogen, carbon monoxide, methane, carbon dioxide and water. The gas contains also small amounts of impurities, like particulates, tars, alkali compounds, sulphur compounds, and halogen compounds. These compounds are often harmful for downstream equipment. Therefore, the gas needs to be cleaned. The needed gas cleaning depends on the application. The application of low temperature fuel cells, as considered in this paper, requires the almost complete removal of harmful components. After gas cleaning the gas can either be directly applied or further processed. When hydrogen is the desired product, as in this paper, further processing can be performed to increase the amount of hydrogen in the gas. Methane can be reformed and carbon monoxide can be converted via the water gas shift reaction. Also the further purification of the produced hydrogen is an option.

Fuel cells are considered to be highly efficient energy converters. Most fuel cells convert electrochemically hydrogen into water, during this conversion electricity is produced and also some additional heat. There are different types of fuel cells available; they all have their own operating window. The proton exchange membrane fuel cell also known as the PEM fuel cell operates at a temperature of 80 °C. This low operating temperature makes it applicable in a domestic setting. Because of the low operating temperature, it generates low temperature heat as a by-product that can be used for space heating.

The combination of biomass gasification and fuel cells is the subject of many studies, like [2–25]. Most of the studies focus on the

* Corresponding author. Tel.: +31 15 2782153; fax: +31 15 2782460.
E-mail address: R.Toonssen@TUDelft.NL (R. Toonssen).

0378-7753/$ – see front matter © 2009 Elsevier B.V. All rights reserved.
doi:10.1016/j.jpowsour.2009.05.044

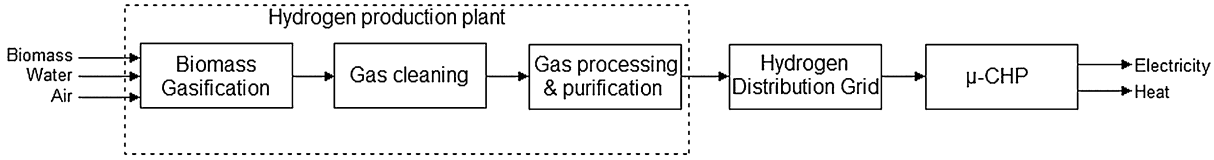

Fig. 1. Schematic overview of the conversion chain.

integration of biomass gasification and high temperature fuel cells, like the studies of Kivisaari et al. [2] and Lobachyov and Richter [6] which focus on biomass gasification and molten carbonate fuel cells (MCFC) for large scale electricity generation. Also studies on small scale electricity generation via biomass gasification and MCFC are presented, like the studies of McIlveen-Wright et al. [3], Donolo et al. [5] and Morita et al. [13].

Many studies are devoted to systems of biomass gasification and solid oxide fuel cells (SOFC). The SOFC is often combined with a gas turbine to form a hybrid system. As in the systems with a MCFC varies the scale from small scale 1 kW_e [9] to large scale 21 MW_e [8] or 30 MW_e [20].

Only very few studies are focussing on the application of biomass gasification and PEM fuel cells, like the study of Ersoz et al. [24] and the study of Sordi et al. [25]. In the study of Ersoz et al. [24] a fixed bed gasifier followed by reforming and cleaning units is coupled to a PEM fuel cell. The influence of the hydrocarbon properties, the gasification parameters and the reforming parameters on system efficiency has been tested.

In the study of Sordi et al. [25], the influence of the syngas composition on the gas processing and on the electricity generation in a PEM fuel cell is investigated.

The application of fuel cells in micro-combined heat and power is widely researched. Most of these micro-CHP systems are fuelled with natural gas. The micro-CHP systems based on PEM fuel cells include desulphurization, reforming, water gas shift reactors and deep carbon monoxide cleaning. An example of such a system can be found in the work of Gigliucci et al. [26].

In this paper the CHP system is fuelled with hydrogen. There are few studies on CHP systems based on PEM fuel cells fuelled with hydrogen. Saidi et al. [27] performed an exergy analysis on a hydrogen fuelled PEM fuel cell CHP system. They found that high voltage operation reduces the irreversibilities in the system.

In a study of Colella [28] some control strategies for a CHP fuel cell system are evaluated with a special focus on the afterburner sub-system.

In a recent study by Page and Krumdieck [29] several energy conversion chains have been evaluated. One of the evaluated chains was the central production of hydrogen via coal gasification, which is distributed in a hydrogen grid and finally used in PEM fuel cell micro-CHPs. They calculated chain efficiencies, on basis of higher heating value of the coal, of 21.8% thermal and 26.2% electrical [29]. However, these efficiencies are not based on detailed system modelling.

In this paper two hydrogen production plants based on biomass are designed. One plant is producing a gaseous fuel with 60% hydrogen, and the other plant is producing 99.99% pure hydrogen. The produced hydrogen is assumed to be pumped into a hydrogen distribution grid, which supplies hydrogen to households. In the household the hydrogen is converted into electrical power and heat. To produce heat and electrical power from hydrogen a micro-combined heat and power (μ-CHP) system based on a PEM fuel cell is used. The electrical power demand in an average household is usually not exceeding 1 kW. Therefore, the maximum electrical power output of the μ-CHP system is set to 1 kW. An exergy analysis has been performed on both the hydrogen plants and on the μ-CHP system. The results of this analysis are combined to evaluate the whole conversion chain from biomass into electricity.

The heat production of the PEM fuel cell has a low quality, due to its low operating temperature. The generated heat is not sufficient to fulfil the heat demand of an average dwelling. Therefore, two additional μ-CHP systems based on PEM fuel cells have been considered. These systems produce 1 kW of electrical power and are also able to generate 3 kW of heat. For that purpose one of the additional μ-CHP systems has a fuel by-pass to a boiler to produce additional heat; the other is connected to a ground coupled electrical driven heat pump. Exergy losses are calculated for all system alternatives and a comparison of the losses is presented.

2. System configurations

The whole chain from biomass to electricity consists of three main parts: the centralized hydrogen production plant, the hydrogen distribution grid and the μ-CHP system. In Fig. 1 a schematic representation is given of the chain from biomass to electricity. In the next sections each part of the chain will be discussed separately, starting with the hydrogen production plant.

2.1. Hydrogen production plant

The hydrogen production plants can be sub-divided into three sections. The first section is the biomass gasification, the second section is the gas cleaning and the final section is the gas processing and purification.

2.1.1. Gasification

The hydrogen plants are supposed to be based on the Fast Internal Circulating Fluidized Bed (FICFB) gasifier. The FICFB gasifier is designed by the Institute of Chemical Engineering and AE Energietechnik. This is an indirect steam gasifier, which means the heat required for the endothermic gasification reactions is supplied by a coupled combustor. The gasifier consists of two fluidized beds, one bubbling bed and one circulating fluidized bed. In the bubbling bed the biomass is gasified with steam at a temperature of around 800 °C, in the circulating fluidized bed the residual char from the gasification is combusted with air at a temperature of 900–1000 °C. The bed material is circulated between the two beds and is used as heat transport medium. The operating pressure is near atmospheric. More information on the FICFB can be found in Refs. [30–34]. This type of gasifier is chosen because it produces a hydrogen rich gas, which results in a high hydrogen yield [35].

2.1.2. Gas cleaning

The gas produced by the gasifier contains several impurities like particulates (5000–10,000 mg Nm^{-3} [33]), tars (1500–4500 mg Nm^{-3} [33]), sulphur compounds (20–50 ppm[1] [33]), nitrogen compounds (ammonia 1000–2000 ppm [33]), halogen

[1] The values are measured after the systems gas cleaning. There is no dedicated sulphur removal in the gas cleaning, so is assumed the values will not deviate much from the measured values.

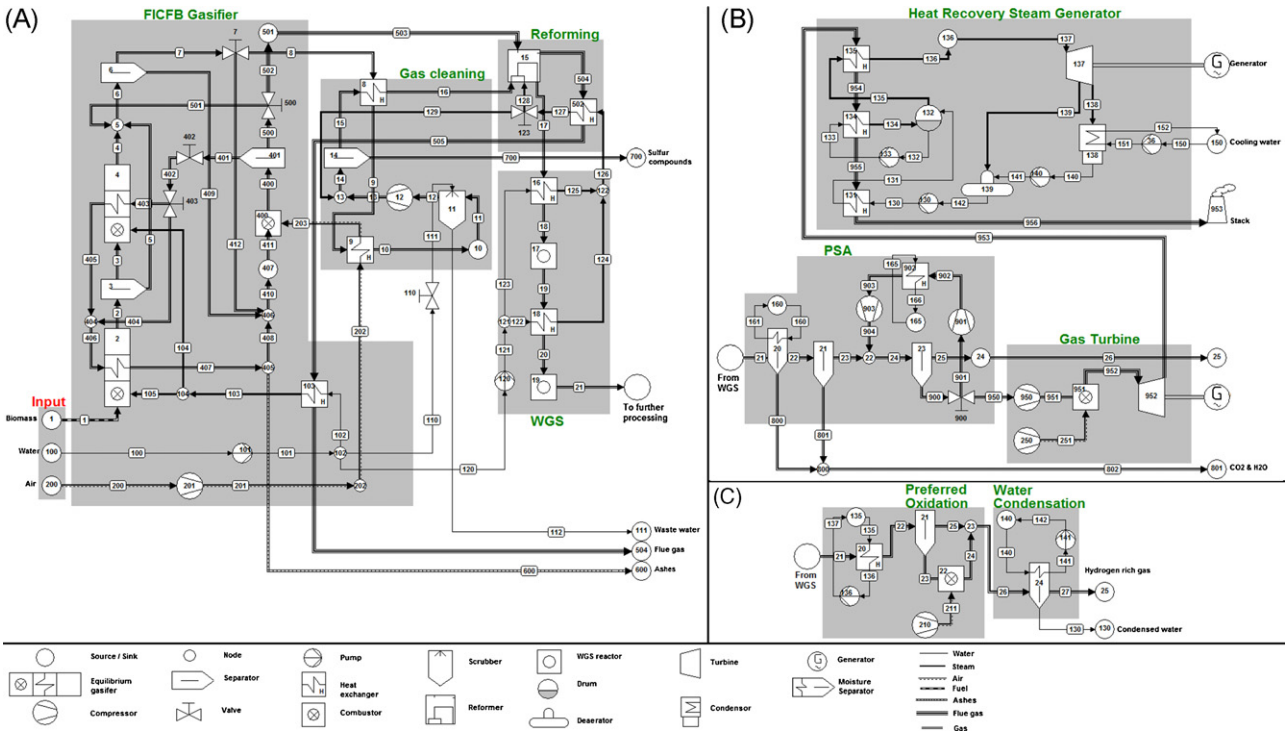

Fig. 2. Flow sheets of the hydrogen plants. The combination of A and C gives hydrogen1 and the combination of A and B gives hydrogen2.

compounds and alkali metals [36,37]. The tars, alkali metals and particulates have the tendency to stick to cold surfaces or cause blockages in all kinds of equipment. These compounds as well as the other impurities have a deteriorating effect on catalytic driven processes as needed for gas processing and final utilization; therefore the impurities have to be removed in a gas cleaning system.

In the gas cleaning system, the producer gas is cooled in two heat exchangers to a temperature of about 120 °C (see Fig. 2A). The alkali metal compounds and some of the tars will condense on the entrained particles [1]. When keeping the superficial gas velocity high in the heat exchangers the abrasive nature of the gas will keep the walls of the heat exchangers clean. The cooled gas is filtered in a bag filter before the gas is cleaned in a water scrubber, in which halogen compounds, nitrogen containing compounds, the residual tars and alkali metal compounds are removed. The scrubber has also a quenching effect on the gas, resulting in a temperature drop to 60 °C. After scrubbing, the producer gas is compressed to a pressure of 36 bar. The resulting reduction of the gas volume enables smaller equipment downstream. Before the gas is passed through an amount of steam is added, to make sure no carbon will deposit in the heat exchangers. Since carbon can deposit when synthesis gas is cooled or heated, if the water content of the gas is low or the rate of temperature change is low, as illustrated by Aravind et al. [22]. Then the gas is passed through a packed bed filled with zinc titanate, in order to remove traces of hydrogen sulphide in the gas. The regeneration of the sorbent is not considered, because it is an exothermic process that will hardly require any energy. After the sulphur removal, the gas is reheated in a heat exchanger with the heat of the raw producer gas coming from the gasification unit.

There are many uncertainties regarding the gas cleaning, especially the scrubber. The effects of the scrubber on the tar and halogen content are not certain. But due to the low operating temperature it is most likely that only light tar compounds are present in the gas.

2.1.3. Gas processing and purification

The gas processing starts with methane reforming followed by the water gas shift. Methane reforming is supposed to take place in a steam reformer. The hot flue gasses coming from the gasification unit are used to supply heat to the reformer. The steam required for the reforming process is produced with the excess heat from the hydrogen plant. The steam to carbon ratio in the reformer is kept above 2.5. This value is sufficient to prevent carbon deposition [38]. The reformer is operated at a pressure of 35 bar and a temperature of 825 °C. The gas coming from the reformer is cooled to 400 °C, before it enters the high temperature water gas shift (WGS) reactor. After the high temperature WGS reactor, the gas is cooled to 210 °C at this temperature it enters the low temperature WGS reactor. The amount of carbon monoxide in the gas is reduced to 0.5–1 vol% [39,40].

After this process step two different gas processing and purification approaches have been considered, leading to two different product qualities and hydrogen production plant designs. In the first approach, called hydrogen1, the gas is further processed in a preferential oxidation unit, in order to remove the residual carbon monoxide from the gas. This unit operates at a temperature of about 135 °C. Besides the carbon monoxide also a small amount of hydrogen is combusted. It is assumed that almost all the carbon monoxide is combusted resulting in a CO concentration below 10 ppm. This is currently not the case, but it is expected that with future developments it will be possible.

After the preferential oxidation, the hydrogen gas is cooled to condense the water vapour in the gas. This results in a hydrogen rich gas with a purity of approximately 60%. Other compounds in the gas are carbon dioxide, methane, and nitrogen. It is assumed that the gas from this process is suitable for a PEM fuel cell; most of the compounds in the gas just act as diluents except for carbon dioxide. It is known that carbon dioxide can cause a decrease in the performance of a PEM fuel cell [41–43]. When using a PEM fuel cell specially suited for reformates, the decrease in performance of the fuel cell will be smaller than for a standard PEM fuel cell [44].

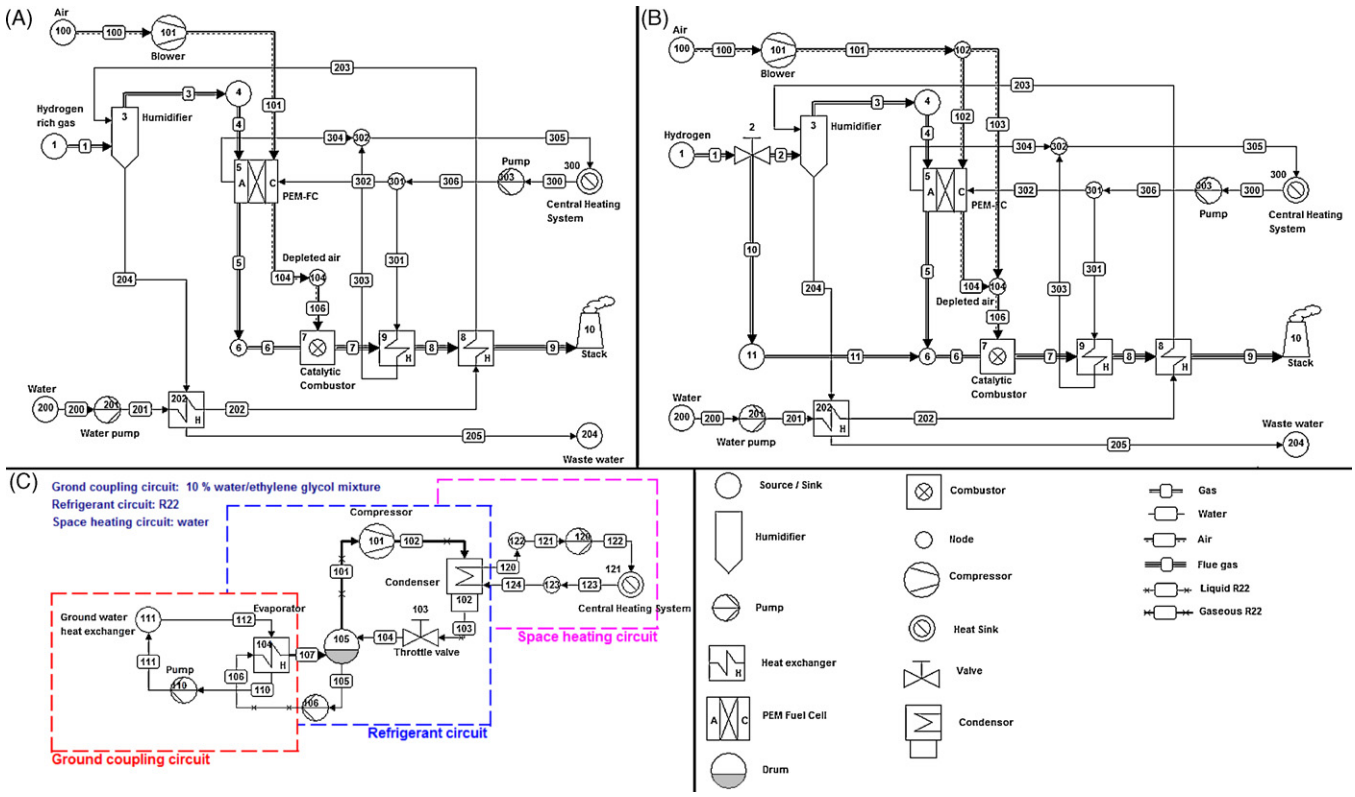

Fig. 3. The flow sheet A is of PEM1; B is the flow sheet of PEM2; A and C combined gives the flow sheet of PEM3.

In the second approach, called hydrogen2, the gas is further processed in a pressure swing adsorption (PSA) unit (see Fig. 2B). First, water is condensed by cooling the gas to 30 °C. Then the gas is fed to the PSA unit where first CO_2 and residual water is removed, then in a second unit the other substances like nitrogen are removed from the gas. For the removal of CO_2 and water a different sorbent is used than for the other compounds. Therefore, a two step process has been chosen. The waste gas coming from the PSA unit contains significant amounts of hydrogen, CO and CH_4. Therefore, the waste gas is combusted in a gas turbine system connected to a generator that produces electricity. The hot flue gasses coming from the gas turbine are used in a bottoming steam turbine cycle in order to produce additional electricity. In this way most of the electrical power necessary to operate the plant can be generated.

2.1.4. Hydrogen transport and distribution

In this paper it is assumed that a hydrogen grid is available. This grid would probably consist of a high pressure part at pressures between 60 and 80 bar for long distance transport; a medium pressure grid (pressures of approximately 20 bar) for large consumers; and low pressure grid (pressure ±5 bar) for domestic application. It is assumed that the hydrogen production plants should feed into the high pressure grid. Eventually the hydrogen will be available at the domestic level. The compression energy to feed hydrogen into the transport grid is fully taken into account. However, energy recovery at expansion to medium pressure or to distribution pressure is not taken into account.

The 60% hydrogen will require a larger diameter piping than the 99.99% pure hydrogen for the transport of the same fuel power. Also the compression power required to compress the 60% hydrogen will be higher than for the 99.99% pure hydrogen.

2.1.5. μ-CHP

The μ-CHP is based on a PEM fuel cell with water cooling. The fuel cell is initially designed to generate 1 kW of electrical power. Due to the limited electrical efficiency of the PEM fuel cell unit also an amount of heat is produced at a temperature sufficient to generate hot water for space heating. In this system (see Fig. 3A) hydrogen is first humidified before it enters the anode of the fuel cell stack. A blower is used to feed air to the cathode of the fuel cell stack. The off-gasses from the anode contain still some hydrogen and are catalytically combusted in an afterburner using air coming from the cathode. Heat is extracted from the hot flue gasses coming from the combustor as well as from the cooling system of the fuel cell stack. This heat is used for space heating and for humidification. This μ-CHP system alternative without additional heat generation and used for the initial calculations is called PEM1.

The initial μ-CHP system PEM1 only produces about 1.9 kW of heat. However, in a domestic setting the heat demand for space heating is often higher than 1.9 kW. Assuming a maximum heat demand of 3 kW, the μ-CHP system needs to be modified to meet this higher heat demand. Two different design options have been considered. The first uses a hydrogen by-pass of the fuel cell, so additional hydrogen is directly combusted in the catalytic combustor. This enables the production of additional hot water for the space heating system. This system option is called PEM2 (see Fig. 3B).

The second system option (called PEM3) generates a little more electricity to power an electrical driven ground coupled heat pump, which supplies the extra heat required. The ground coupled heat pump consist of three circuits, the ground coupling circuit; the refrigerant circuit and the space heating circuit (see Fig. 3C). The cycle that extracts heat from the soil uses a 10% ethylene glycol/water mixture as working fluid. The cycle transfers heat from the ground water to the refrigerant circuit. The working fluid for the

Table 1
Dry composition of the used biomass [35,50].

	Amount	Unit
Carbon (C)	49.97	wt%
Hydrogen (H)	6.12	wt%
Oxygen (O)	42.49	wt%
Nitrogen (N)	0.55	wt%
Sulphur (S)	0.06	wt%
Ash (SiO_2)	0.80	wt%
Lower heating value (dry)	18,620	kJ kg^{-1}
Exergy (dry)	20,611	kJ kg^{-1}

refrigerant circuit is R22. Heat extracted from the ground coupled circuit is used to evaporate it. The evaporated R22 is compressed to 26 bar and condensed in a condenser that transfers heat to the space heating circuit. After the condensation of R22, it is throttled to a lower pressure (4.8 bar) and evaporated again. The space heating cycle is similar to the one of the PEM1 system; water of 65 °C is used for space heating. The cooled return water (45 °C) is heated in the condenser of the refrigerant cycle. The coefficient of performance of the heat pump is 3.21.

In Fig. 3, the flow sheets of the three μ-CHP system alternatives are given. PEM1 is represented by Fig. 3A, PEM2 by Fig. 3B and PEM3 by a combination of Fig. 3A and C.

The space heating system uses hot water of 65 °C for heating. When the water leaves the space heating system for reheating, it has a temperature of 45 °C. The pressure of the water in this system is 1.5 bar.

The electrical power and heat demand of houses are continuously fluctuating; then the μ-CHP system will continuously cycle between full and part load. However, for a first estimate all calculations in this paper are based on design load, and the additional effect of fluctuations in demands are not considered. It is expected that the relative differences between the alternatives are sufficiently represented by the conditions at design load.

3. Modelling

The designed systems have been modelled using the computer program Cycle-Tempo [45], a flow sheeting program developed for the evaluation of energy conversion systems. The computer program Cycle-Tempo is available for commercial application since 1983. Many universities, research organizations, engineering companies and industries worldwide are using the program.

A model has been created for both hydrogen production plants. Separate models have been made for the three μ-CHP systems. By combining the results of a hydrogen production plant model and a μ-CHP model a first impression of the performance of the whole chain of power production can be given. Some general assumptions have been made:

- The systems are operated in steady state.
- The thermal input of the gasifier is approximately 70 MW.
- The heat exchangers are operated in counter current flow.
- There is no fouling caused by tars and/or alkali metal compounds.
- The gas cleaning systems are able to achieve the required gas purity.
- Processes are adiabatic.
- The mechanical efficiency of all rotary equipment is 99%.

The biomass used in the calculations is A-quality wood with a moisture content 25.2 wt% on dry basis; the dry composition of the biomass is given in Table 1.

The modelling of the biomass gasification is done in such a way that the mass and energy balances are closed. The composition of the producer gas found in literature is used to tune the gasification model [35]. The model of the gasifier uses two equilibrium gasifiers in series, which calculate the gas composition by Gibbs free energy minimization for different equilibrium temperatures and pressures (see Fig. 2). The first equilibrium gasifier is mainly used for the production of methane. During the calculation of the equilibrium 22 mol% of carbon is excluded. The separator (nr. 3) behind the first gasifier (nr. 2) is used to by-pass some of the components resulting from the first gasifier. The remaining mixture is passed to the second gasifier (nr. 4). The final composition can be tuned by controlling the operating conditions of the gasifiers and the separated components. Also a small amount (3 vol%) of flue gas from the combustion part of the FICFB is mixed with the gas. The cyclone for the removal of solids is modelled with a separator; it removes the ashes and carbon from the gas. The removed solids are mixed with the bed material and with some (20 wt%) producer gas, this mixture is combusted. The solids are separated in a separator and used to supply heat to the gasifiers.

The calculation of the reforming and water gas shift reactions is also based on the minimization of the Gibbs free energy. It is assumed that these processes reach equilibrium.

In Tables 2 and 3, the input data for the different model components depicted in Figs. 2 and 3 can be found.

The PEM fuel cell model available in Cycle-Tempo is used to calculate the performance of the system. The active cell area and the current flow I are calculated from the specified current density, cell voltage V and electrical power output P_e. It is supposed that the processes occur at constant temperature and pressure. The fuel flow to the fuel cell $\Phi_{m,a,in}$ relates to the total current as given by the following equation:

$$I = \frac{\Phi_{m,a,in}}{M_a} 2F y^0_{H_2} U_F \tag{1}$$

Here $y^0_{H_2}$ is the hydrogen concentration at the inlet, M_a is the molar mass of the anode gas, F is the Faraday constant and U_F is the fuel utilization. The mass flow of protons through the membrane is calculated based on the current flow. With the mass flow of protons and the oxygen utilization, the airflow to the fuel cell is calculated. An energy balance is used to calculate the amount of cooling water required to keep the fuel cell at the set outlet temperature.

For the equivalent cell resistance a one-dimensional model is used. The temperatures, pressures and composition are supposed to be constant in a cross-section perpendicular to the direction of the fuel flow in the fuel cell. For the cross-section, the reversible cell voltage $V_{rev,x}$ is determined with the Nernst equation assuming ideal gas and gaseous water as a product:

$$V_{rev,x} = V^0_{rev} + \frac{RT}{2F} \ln\left(\frac{y_{H_2} y^{1/2}_{O_2,c}}{y_{H_2O,c}} \cdot P^{1/2}_{cell} \right) \tag{2}$$

where V^0_{rev} is the standard reversible voltage for hydrogen, R is the universal gas constant, T the temperature, y the mole fraction at the cross-section, and P is the pressure. In the model, it is assumed that the voltage losses on the level of the electrodes are negligible in the x-direction. This means that the cell voltage is supposed to be constant over the fuel cell. So, the voltage loss ΔV_x can be calculated using the following equation:

$$\Delta V_x = V_{rev,x} - V \tag{3}$$

Then the equivalent fuel cell resistance R_{eq} is

$$R_{eq} = \frac{\Delta V_x}{i_x} \tag{4}$$

where i_x is the current density.

Table 2
Input parameters of the models for hydrogen production (pressures are given in bar and temperatures in degrees Celcius).

No.	Description	Input
Gasifier		
2	Gasifier	$P_r = 1$, $T_r = 180$, S/F = 0.2, $P_{out} = 1.47$, $T_{out} = 800$
3	Separator	$\Delta P = 0$, $\Delta T = 0$
4	Gasifier	$P_r = 2000$, $T_r = 2000$, S/F = 0.143, $P_{out} = 1.47$, $T_{out} = 800$
5	Node	$\Delta P = 0$
6	Separator	$\Delta P = 0.01$, $\Delta T = 0$, C: 100%, SiO_2: 100%
7	Valve	$\Delta P = 0$, 20% mass flow pipe 7 to pipe 412
101	Pump	$P_{out} = 1.5$, $\eta_i = 0.75$
102	Node	$\Delta P = 0$
104	Node	$\Delta P = 0$
201	Compressor	$P_{out} = 1.49$, $\eta_i = 0.80$
202	Node	$\Delta P = 0$
400	Combustor	$P_r = 1$, $T_r = 180$, $\lambda = 1.1$
401	Separator	$\Delta P = 0.01$, $\Delta T = 0$, SiO_2: 100%
402	Valve	$\Delta P = 0$, mass flow pipe 402 18.3 kg s^{-1}
403	Valve	$\Delta P = 0$, 80% mass flow pipe 402 to pipe 403
404	Node	
405	Node	$\Delta P = 0.01$
406	Node	$\Delta P = 0$
407	Sink/source	$\Delta P = 0$, Est. $T_{out} = 1000$, WFOT = 90
500	Valve	$\Delta P = 0$, 0.3% volume flow pipe 500 to pipe 501
501	Sink/source	$\Delta P = 0$, $\Delta T = 0$
Gas cleaning		
8	Heat exchanger	$\Delta P_C = 0.72$, $\Delta P_H = 0.0292$, $\Delta T_{pinchH} = 50$
9	Heat exchanger	$\Delta P_C = 0.3$, $\Delta P_H = 0.0286$, $\Delta T_{Cout} = 546.81$
10	Sink/source	$\Delta P = 0.028$, $\Delta T = 0$
11	Scrubber	$\Delta P_{gas} = 0.0269$, $T_{ingas} = 120$,
12	Compressor	$P_{out} = 36.6$, $\eta_i = 0.80$
13	Node	$\Delta P = 0$
14	Separator	$\Delta P = 0.7164$
110	Valve	$\Delta P = 0.03$, 5× mass flow pipe 12 for pipe 111
Reformer		
15	Reformer	$P_r = 32.23$, $T_r = 825$, S/F = 0.333, $\Delta P_1 = 0.68$, $\Delta P_1 = 0.03$, $T_{out} = 800$
103	Heat exchanger	$\Delta P_C = 0.03$, $\Delta P_H = 0.282$, $\Delta T_{Cout} = 400$
123	Valve	$\Delta P = 0$, 1.6325 mass flow to pipe 129
502	Heat exchanger	$\Delta P_C = 0.68$, $\Delta P_H = 0.03$, $\Delta T_{Cout} = 600$
WGS		
16	Heat exchanger	$\Delta P_C = 0.7$, $\Delta P_H = 0.66$, $\Delta T_{Hout} = 380$
17	Reactor	$\Delta P = 0.64$, $T_{WGS} = 400$
18	Heat exchanger	$\Delta P_C = 0.7$, $\Delta P_H = 0.66$, $\Delta T_{Hout} = 210$, $T_{Cout} = 250$
19	Reactor	$\Delta P = 0.62$, $T_{WGS} = 220$
120	Pump	$P_{out} = 38.48$, $\eta_i = 0.75$
121	Node	$\Delta P = 0$
122	Node	$\Delta P = 0$
PSA (Hydrogen2)		
20	Moisture separator	$\Delta P_C = 0$, $\Delta P_H = 0.62$, $\Delta T_{Cout} = 20$, $\Delta T_{Hout} = 25$
21	Separator	$\Delta P_1 = 0.62$, $\Delta P_2 = 30$, $\Delta T = 0$, CO_2: 100%, H_2O: 100%
22	Node	$\Delta P = 0$
23	Separator	$\Delta P_1 = 0.6$, $\Delta P_2 = 29.6$, $\Delta T = 0$, other: 99.99%, H_2: 16%
24	Sink/source	$\Delta P = 0$, Est. $T_{out} = 25$
160	Sink/source	$P_{out} = 1.01325$, $T_{out} = 15$
165	Sink/source	$P_{out} = 1.01325$, $T_{out} = 15$
800	Node	$\Delta P = 0$
900	Valve	$\Delta P = 0$, 78% mass flow pipe 900 to pipe 901
901	Compressor	$P_{out} = 4.75$, $\eta_i = 0.80$
902	Heat exchanger	$\Delta P_C = 0$, $\Delta P_H = 0.095$, $\Delta T_{Cout} = 20$, $\Delta T_{Hout} = 30$
903	Compressor	$P_{out} = 30.6$, $\eta_i = 0.80$
Gas Turbine (Hydrogen2)		
250	Compressor	$P_{out} = 9$, $\eta_i = 0.80$
950	Compressor	$P_{out} = 9$, $\eta_i = 0.80$
951	Combustor	$\Delta P = 0.18$, $P_r = 9$, $T_r = 1200$, $\lambda = 2.2$
952	Turbine	$\eta_i = 0.90$
Heat recovery steam generator (Hydrogen2)		
36	Pump	$P_{out} = 1.21325$, $\eta_i = 0.75$
130	Pump	$\eta_i = 0.75$
131	Heat exchanger	$\Delta P_C = 1$, $\Delta P_H = 0.02$, $\Delta T_{pinchC} = 10$
132	Drum	CRATIO = 4
133	Pump	$\eta_i = 0.75$
134	Heat exchanger	$\Delta P_C = 1$, $\Delta P_H = 0.02$, $\Delta T_{pinchC} = 20$
135	Heat exchanger	$\Delta P_C = 1$, $\Delta P_H = 0.02$, $T_{outC} = 540$
136	Sink/source	$\Delta P = 1.2$, $\Delta H = -2$
137	Turbine	$P_{in} = 80.2$, $\eta_i = 0.882$
138	Condensor	$P_{out} = 0.03$, $T_{outC} = 19$, $\Delta P_C = 0.2$
139	Deaerator	$P_{in} = 1.01325$, $\Delta P = 0$
140	Pump	$\eta_i = 0.75$
150	Sink/Source	$P_{out} = 1.01325$, $T_{out} = 12$
Preferential oxidation (Hydrogen1)		
20	Heat exchanger	$\Delta P_C = 0.1$, $\Delta P_H = 0.6$, $T_{outH} = 135$, $T_{outC} = 20$
21	Separator	$\Delta P_1 = 0.62$, $\Delta P_2 = 0$, $\Delta T = 0$, CO: 100%, H_2: 0.7%
22	Combustor	$\Delta P = 0.62$, $P_r = 30.61$, $T_r = 135$, $\lambda = 1$
23	Node	$\Delta P = 0$
135	Sink/source	$P_{out} = 1.1325$, $T_{out} = 15$, $\Delta P = 0.1$
136	Pump	$\eta_i = 0.75$
210	Compressor	$P_{out} = 31.22$, $\eta_i = 0.80$
Condensation (Hydrogen1)		
24	Moisture separator	$\Delta P_C = 0.1$, $\Delta P_H = 0.6$, $T_{outH} = 25$, $T_{outC} = 20$
140	Sink/Source	$P_{out} = 1.1325$, $T_{out} = 15$, $\Delta P = 0.1$
141	Pump	$\eta_i = 0.75$

Table 3
Input parameters for the models of the μ-CHP systems (pressures are given in bar and temperatures in degrees Celcius).

No.	Description	Input
PEM1		
1	Sink/source	$P_{out} = 1.56$, $T_{out} = 15$
3	Humidifier	$\Delta P_G = 0.03$, $T_{outG} = 67$, $\Delta P_W = 0.03$, $T_{outW} = 67$, RELHUM = 1
4	Sink/source	$\Delta P = 0$, $\Delta T = 0$
5	Fuel cell	SPFC, $\Delta P_{an} = 0.03$, $\Delta P_{cat} = 0.03$, $T_{out} = 80$, DCAC = 0.965, $P_{FC} = 1.5$, $T_{FC} = 80$, $U_F = 80\%$, $U_{ox} = 50\%$, $\Delta P_C = 0.03$
6	Node	$\Delta P = 0$
7	Combustor	$\Delta P = 0.03$, $T_r = 750$, $P_r = 1.47$
8	Heat exchanger	$\Delta P_C = 0.031$, $T_{outC} = 80$, $\Delta P_H = 0.03$
9	Heat exchanger	$\Delta P_C = 0.031$, $T_{outC} = 65$, $\Delta P_H = 0.03$
10	Stack	$T_{in} = 80$
100	Sink/source	$P_{out} = 1.01325$, $T_{out} = 15$
101	Compressor	$P_{out} = 1.53$, $\eta_i = 0.8$
104	Node	$\Delta P = 0$
200	Sink/source	$P_{out} = 1.01325$, $T_{out} = 15$, $\phi_m = 1.1$
201	Pump	$P_{out} = 1.593$, $\eta_i = 0.75$
202	Heat exchanger	$\Delta P_C = 0.031$, $\Delta T_{pinchC} = 5$, $\Delta P_H = 0.03$
204	Sink/Source	
300	Heat Sink	$P_{out} = 1.5$, $\Delta P = 0.03$, $T_{in} = 65$, $T_{out} = 45$
301	Node	$\Delta P = 0$
302	Node	$\Delta P = 0$
303	Pump	$P_{out} = 1.593$, $\eta_i = 0.75$
PEM2		
1	Sink/source	$P_{out} = 1.56$, $T_{out} = 15$
2	Valve	$\Delta P = 0.03$, 24.8% mass flow pipe 1 to pipe 10
3	Humidifier	$\Delta P_G = 0.03$, $T_{outG} = 67$, $\Delta P_W = 0.03$, $T_{outW} = 67$, RELHUM = 1
4	Sink/source	$\Delta P = 0$, $\Delta T = 0$
5	Fuel cell	SPFC, $\Delta P_{an} = 0.03$, $\Delta P_{cat} = 0.03$, $T_{out} = 80$, DCAC = 0.965, $P_{FC} = 1.5$, $T_{FC} = 80$, $U_F = 80\%$, $U_{ox} = 50\%$, $\Delta P_C = 0.03$
6	Node	$\Delta P = 0$
7	Combustor	$\Delta P = 0.03$, $T_r = 1200$, $P_r = 1.47$, $\lambda = 3.5$
8	Heat exchanger	$\Delta P_C = 0.031$, $T_{outC} = 80$, $\Delta P_H = 0.03$
9	Heat exchanger	$\Delta P_C = 0.031$, $T_{outC} = 65$, $\Delta P_H = 0.03$
10	Stack	$T_{in} = 80$
11	Sink/source	$\Delta P = 0.06$, $\Delta T = 0$
100	Sink/source	$P_{out} = 1.01325$, $T_{out} = 15$
101	Compressor	$P_{out} = 1.53$, $\eta_i = 0.8$
104	Node	$\Delta P = 0$
200	Sink/source	$P_{out} = 1.01325$, $T_{out} = 15$, $\phi_m = 1.1$
201	Pump	$P_{out} = 1.593$, $\eta_i = 0.75$
202	Heat exchanger	$\Delta P_C = 0.031$, $\Delta T_{pinchC} = 5$, $\Delta P_H = 0.03$
204	Sink/source	
300	Heat sink	$P_{out} = 1.5$, $\Delta P = 0.03$, $T_{in} = 65$, $T_{out} = 45$
301	Node	$\Delta P = 0$
302	Node	$\Delta P = 0$
303	Pump	$P_{out} = 1.593$, $\eta_i = 0.75$

Table 3 (*Continued*)

No.	Description	Input
PEM3		
1	Sink/source	P_{out} = 1.56, T_{out} = 15
2	Humidifier	ΔP_G = 0.03, T_{outG} = 67, ΔP_W = 0.03, T_{outW} = 67, RELHUM = 1
3	Sink/source	ΔP = 0, ΔT = 0
4	Fuel cell	SPFC, ΔP_{an} = 0.03, ΔP_{cat} = 0.03, T_{out} = 80, DCAC = 0.965, P_{FC} = 1.5, T_{FC} = 80, U_F = 80%, U_{ox} = 50%, ΔP_C = 0.03
5	Combustor	ΔP = 0.03, T_r = 1200, P_r = 1.47
6	Heat exchanger	ΔP_C = 0.031, T_{outC} = 65, ΔP_H = 0.03
7	Heat exchanger	ΔP_C = 0.031, T_{outC} = 80, ΔP_H = 0.03
8	Stack	T_{in} = 80
50	Sink/source	P_{out} = 1.01325, T_{out} = 15
51	Compressor	P_{out} = 1.53, η_i = 0.8
52	Node	ΔP = 0
70	Heat sink	P_{out} = 1.5, ΔP = 0.03, T_{in} = 65, T_{out} = 45
71	Node	ΔP = 0
72	Node	ΔP = 0
73	Pump	P_{out} = 1.593, η_i = 0.75
80	Sink/source	P_{out} = 1.01325, T_{out} = 15, ϕ_m = 1.1
81	Pump	P_{out} = 1.593, η_i = 0.75
82	Heat exchanger	ΔP_C = 0.031, ΔT_{pinchC} = 5, ΔP_H = 0.03
83	Sink/source	
101	Compressor	P_{out} = 26, η_i = 0.8
102	Condenser	ΔP_C = 0.03, T_{outH} = 60, ΔP_H = 0.52
103	Valve	ΔP = 20.68, mass flow pipe 104 = 3.975
104	Heat exchanger	ΔP_C = 0.096, T_{outC} = 3, ΔP_H = 0.02, T_{outH} = 6.8
105	Drum	
106	Pump	η_i = 0.75
110	Pump	P_{out} = 1.05325, η_i = 0.75
111	Sink/source	ΔP = 0.02, T_{out} = 8
120	Pump	P_{out} = 1.593, η_i = 0.75
121	Heat sink	P_{out} = 1.5, ΔP = 0.03, T_{in} = 65, T_{out} = 45
122	Node	ΔP = 0
123	Node	ΔP = 0

The equivalent fuel cell resistance can also be defined using the following equation:

$$R_{eq} = \frac{i + i_n}{i} \cdot R_{ohm} + \frac{A}{i} \ln\left(\frac{i + i_n}{i_0}\right) - \frac{B}{i} \ln\left(1 - \frac{i + i_n}{i_l}\right) \quad (5)$$

Here R_{ohm} is the ohmic resistance of the fuel cell, A is the slope of the Tafel line, B is the constant in the mass transfer overvoltage equation, i_n is the internal and fuel crossover equivalent current density, i_0 is the exchange current density and i_l is the limiting current density. The used values can be found in Table 4.

The fuel utilization in the model was set to 80% and the oxygen utilization to 50%. The electrical output of the fuel cell was set in such a way that the net electrical output of the whole μ-CHP system was 1 kW. The conversion of DC to AC is assumed to have an efficiency of 96.5%. The PEM fuel cells are assumed to be suitable for reformate as a fuel, so the CO_2 in the fuel is only considered as a diluent.

Temperature and pressure of the fuel entering the μ-CHP systems are fixed to 15 °C and 1.56 bar, respectively. The air as well as the water used in these μ-CHP systems enter at environmental conditions.

Table 4
Used values for determining the equivalent fuel cell resistance.

Name	Symbol	Value	Unit
Ohmic fuel cell resistance [51]	R_{ohm}	1e−5	Ω m^2
Slope Tafel line	A	0.0484	V
Constant in mass transfer overvoltage equation	B	0.05	V
Internal and fuel crossover equivalent current density	i_n	20	A m^{-2}
Limiting current density	i_l	9000	A m^{-2}
Exchange current density	i_0	0.67	A m^{-2}

Table 5
Composition of the environment [35].

Component	Mole fraction	Component	Mole fraction	Component	Mole fraction
$Al_2O_{3(s)}$	0.01	N_2	76.73	SO_2	0.01
Ar	0.91	O_2	20.60	Cl_2	0.01
CO_2	0.03	$SiO_{2(s)}$	0.01	F_2	0.01
H_2O	1.68				

Cycle-Tempo can perform exergy calculations. Exergy values of all flows considered in the system flow diagram are calculated based on the previously calculated pressure, temperature and chemical composition. The thermo-mechanical (physical) exergy and the chemical exergy are calculated separately. The calculation of chemical exergies requires the definition of an environment that determines the exergy of any considered component at reference conditions. The environment applied for this study is shown in Table 5. Exergy losses are calculated by the program from the exergy balances of the various processes. A more detailed description of the exergy calculations is presented in the book of Szargut et al. [46]. The environmental temperature is supposed to be 15 °C and the environmental pressure 1.01325 bar (1 atm).

The electrical exergy efficiency of the μ-CHP unit is calculated as

$$\eta_{ex,el} = \frac{\sum P_{el,out} - \sum P_{el,in}}{Ex_{fuel,in}} \quad (6)$$

where $P_{el,out}$ is the electrical output of the system, $P_{el,in}$ the electrical input of the system and $Ex_{fuel,in}$ the exergy of the fuel put in the system.

The overall exergy efficiency is given as

$$\eta_{ex,tot} = \frac{\sum P_{el,out} + \sum Ex_{heat,out} - \sum P_{el,in}}{Ex_{fuel,in}} \quad (7)$$

Here $Ex_{heat,out}$ is the exergy of the usable heat produced by the system.

The overall energy efficiency is calculated as

$$\eta = \frac{\sum P_{el,out} + Q - \sum P_{el,in}}{\phi_{m,fuel} \cdot LHV_{fuel}} \quad (8)$$

Here Q is the usable heat produced by the system, $\Phi_{m,fuel}$ the mass flow of fuel in the system and LHV_{fuel} the lower heating value of the fuel.

4. Results

4.1. Hydrogen production

The gasification process converts 4.12 kg s^{-1} of wood together with 1.30 kg s^{-1} water into 4.26 kg s^{-1} syngas with a composition as given in Table 6. The residual char from the gasification is combusted to provide the heat required for the endothermic gasification process. For the combustion is 7.97 kg s^{-1} air fed to the combustor; this is an excess of 10%. The temperature of the syngas leaving the gasifier is 813 °C and the pressure is 1.46 bar. Also a flue gas stream

Table 6
Dry composition of the producer gas compared with literature [32].

Component	Output model [vol%]	Literature data [vol%]
Hydrogen (H_2)	35.22	30–40
Carbon monoxide (CO)	22.63	20–30
Methane (CH_4)	20.86	15–25
Carbon dioxide (CO_2)	17.18	8–12
Nitrogen (N_2)	3.93	1–5
Other	0.18	

Table 7
The final composition of 60% pure hydrogen.

Component	Molar fraction [mol%]
Hydrogen (H_2)	60.76
Methane (CH_4)	3.16
Carbon dioxide (CO_2)	32.39
Water (H_2O)	0.11
Nitrogen (N_2)	3.54
Argon (Ar)	0.04

is leaving the gasification unit at a temperature of 1237 °C and the same pressure as the producer gas. The flue gas is utilized for a variety of heating purposes like heating the reformer and steam generation for the gasification process.

The generated producer gas is passed to the gas cleaning system. During the gas cleaning process, the composition of the producer gas is not supposed to change. Only the water content of the gas will change. Much water condenses during the scrubbing process and is removed with the wastewater. The water fraction changes from 34 mol% to 12 mol%. For the scrubbing process, 16 kg s^{-1} water is used, which enters the scrubber at a temperature of 15 °C and a pressure of 1.4 bar. In the pressurization step, gas is compressed to approximately 36 bar. After the compression, 1.6 kg s^{-1} steam is added to increase the water content of the gas. The temperature and pressure of this steam are respectively 600 °C and 35 bar. The compressed gas is then desulphurized and transferred to the reformer. In the reformer, the methane is reformed with 1.6 kg s^{-1} steam, which has a temperature of 600 °C and a pressure of 35 bar. About 70% of the methane is converted in the reformer. After the reforming, the carbon monoxide in the producer gas is converted into hydrogen in a two-stage water gas shift process. The heat extracted during cooling of the gas prior and between the high and low temperature water gas shift is used to produce steam.

4.1.1. Hydrogen1

By combining Fig. 2A and C the flow sheet of the hydrogen1 process can be found.

After the WGS process, the gas is cooled to 135 °C and then treated in a preferential oxidation reactor to remove the residual carbon monoxide from the gas. As assumed, all the carbon monoxide and 0.7 mol% [47] of hydrogen is converted in the reactor. Finally, the gas is cooled to 25 °C in order to condensate large part of the water in the gas. This resulted in a gas composition as given in Table 7. The total mass flow of hydrogen rich gas is 4.2 kg s^{-1}. The whole process consumes 3300 kW of electricity, which has to be imported.

4.1.2. Hydrogen2

The flow sheet for the hydrogen2 process can be obtained by combining Fig. 2A and B.

In the hydrogen2 process, the gas coming from the WGS system is first cooled before it is transferred to the PSA. During the cooling, a large part of the water in the gas is condensed and removed from the gas. First the residual water and the carbon dioxide are removed from the gas by adsorption. Then in the next step all the other impurities, like methane, carbon monoxide and nitrogen, are removed from the gas. This results in 0.3 kg s^{-1} of 99.99% pure hydrogen, a stream of almost 6 kg s^{-1} containing water and CO_2 and a stream of 0.3 kg s^{-1} with all the impurities. This last stream of impurities contains a reasonable amount of combustibles. Therefore, it is applied in a gas turbine for the generation of additional electric power. The hot flue gasses coming from the gas turbine are cooled in a heat recovery steam generator. The produced steam is used in a bottoming cycle to generate electricity. The overall generated electric power is 6189 kW. The whole process consumes 6427 kW of electricity. A small amount of electrical power (239 kW) has to be supplied from outside the plant.

4.1.3. The two hydrogen production plants

The hydrogen (rich) gas produced in both plants is at a pressure of 30 bar and a temperature of 25 °C.

For both hydrogen plants are the exergy efficiencies determined. The exergy efficiency is determined by dividing the exergy of the generated hydrogen (rich) gas flow by the exergy of the biomass plus the imported electrical power input. The exergy efficiency for the hydrogen1 plant is 61.4%. For the hydrogen2 plant the efficiency is 50.5%.

In Fig. 4, the exergy flow diagrams are given for the two hydrogen production plants. The temperature and pressure of the main streams from biomass to hydrogen in the production plant are given in Table 8. The pipe numbers correspond to the pipe numbers in Fig. 2.

4.2. Hydrogen distribution

The hydrogen produced in the hydrogen production plants need to be compressed further to 80 bar. To compress all the 60% hydrogen produced by one hydrogen1 plant will required 859 kW of

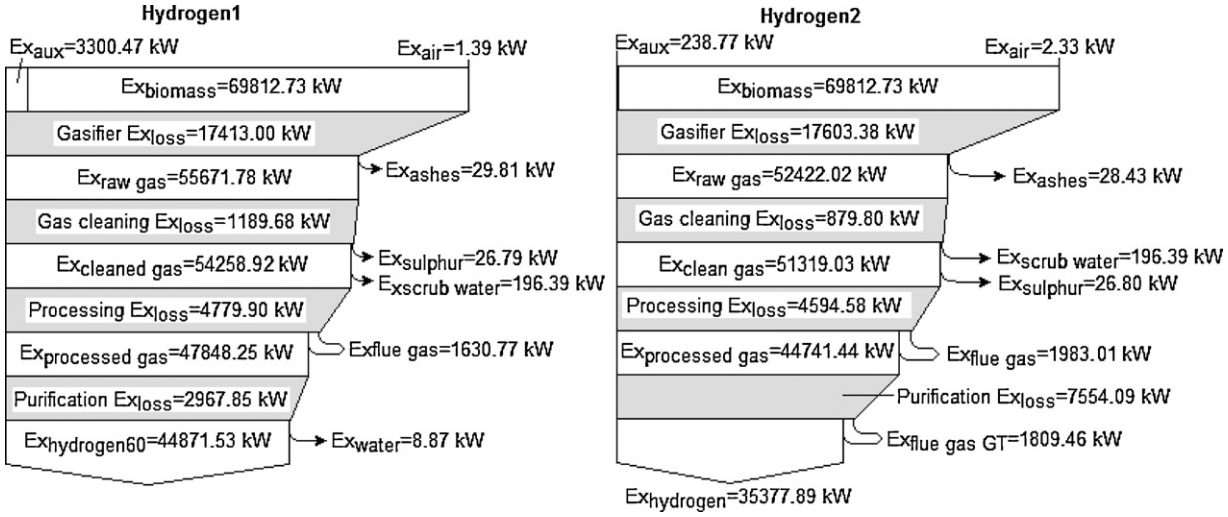

Fig. 4. Exergy flow diagrams of both the hydrogen production plants. The flow diagram on the left is of hydrogen1 and the one on the right is of hydrogen2.

Table 8
Temperatures and pressures for several important pipes within the hydrogen production plants.

Figure 2 part	Pipe number	Pressure [bar]	Temperature [°C]	Figure 2 part	Pipe number	Pressure [bar]	Temperature [°C]
A	8	1.460	813.08	C	22	31.22	135.00
A	9	1.431	617.76	C	26	30.60	143.81
A	10	1.402	120.00	C	27	30.00	25.00
A	12	1.347	56.30	A	110	1.500	15.01
A	13	36.54	528.38	A	112	1.347	56.30
A	14	36.54	551.46	A	502	1.47	1238.67
A	15	35.82	593.20	A	504	1.44	878.78
A	16	35.10	763.08	A	505	1.41	681.41
A	17	34.42	800.00	A	506	1.382	299.07
A	18	33.76	380.00	B	802	1.22	24.69
A	19	33.12	450.03	B	950	1.000	105.95
A	20	32.46	210.00	B	952	8.82	1371.14
A	21	31.22	225.10	B	953	1.073	805.73
B	22	31.22	30.00	B	956	1.013	111.22
B	25	30.00	105.95	C	130	30.00	25.00

electric power. The amount of electric power required for the compression of all the hydrogen produced by one hydrogen2 plant is 512 kW. This compression is supposed to occur in two stages with intercooling. The heat extracted due to the intercooling is assumed to be lost. When the electrical power demand for the compression is added to the electrical power input of the hydrogen plant the efficiencies will drop. For hydrogen1 the exergy efficiency becomes 60.6% and for drogen2 50.1%.

The volume flow of the 60% hydrogen produced by the hydrogen1 plant at 80 bar and a temperature of 15 °C is 265 $m^3\,h^{-1}$. The volume flow of the hydrogen2 plant at similar conditions is 156 $m^3\,h^{-1}$.

4.3. μ-CHP

As mentioned earlier, three different μ-CHP systems have been considered. The first is used as a base case for the calculations, called PEM1. PEM1 will only generate only 1.9 kW of heat. Since it is assumed that the heat demand is 3 kW; additional facilities are necessary to meet this requirement. Two options have been considered for this evaluation: PEM2 and PEM3. Each system is evaluated with two fuels: 60% hydrogen coming from hydrogen1 and 99.99% pure hydrogen coming from hydrogen2. In all the systems the electrical power output of the μ-CHP system is 1 kW.

4.3.1. PEM1

The gross power production of the PEM1 μ-CHP system is 1.07 kW. To produce this amount of power 1.12 kg h^{-1} of 60% hydrogen is required. When using 99.99% pure hydrogen the required amount is 0.09 kg h^{-1}. The calculated cell voltage of the fuel cell using 60% hydrogen is 0.53 V, for 99.99% pure hydrogen this is 0.55 V. The required fuel cell area also differs with the purity of the fuel. When using 60% pure hydrogen the required fuel cell area is 0.26 m^2 and for pure hydrogen it is 0.25 m^2.

The electrical exergy efficiency for the 60% hydrogen and pure hydrogen are respectively 31.0% and 32.1%. The overall exergy efficiencies are found to be 38.3% and 39.7%, respectively. For comparison, the overall thermal efficiencies are 92.4% and 92.8%, respectively. These efficiencies are calculated using Eqs. (6)–(8), respectively.

4.3.2. PEM2

The PEM1 unit, as described before, is not able to generate sufficient heat under all circumstances. As the maximum heat demand is set to 3 kW, the unit needs to be modified in order to enable the generation of all the demanded heat. In the PEM2 system, the additional heat is generated by by-passing some fuel and some air to the boiler of the μ-CHP system, as indicated in Fig. 3B.

For PEM2 some data is given in Table 9. The amount of fuel by-passed is dependant of the purity of the fuel. For 60% hydrogen 25.2% needs to be by-passed and for pure hydrogen this amount is 24.8%. The heat production of the fuel cell causes this difference, because the fuel cell operating on 60% hydrogen produces 1.13 kW and the one on pure hydrogen1.12 kW.

4.3.3. PEM3

In the PEM3 system, a ground coupled heat pump is used to produce additional heat to meet the requirements. In this system the PEM fuel cell produces a little more electricity to power the heat pump, while the net production of electricity remains at 1 kW. In the case that 60% hydrogen is used the amount of additional power is 0.229 kW, for pure hydrogen this amount is 0.224 kW. Only a small portion of the heat is produced by the heat pump, for 60% hydrogen this amount is 0.735 kW and for pure hydrogen it is 0.718 kW. Some other results for the PEM3 system fuelled with both fuels can be found in Table 9.

4.4. The whole chain from biomass to heat and power

To determine the exergy efficiency of the whole chain from biomass to electricity, the exergy efficiency of the hydrogen production including the distribution grid needs to be multiplied by the electrical exergy efficiency of the μ-CHP. For the exergy efficiency of the whole chain from biomass to electricity and heat, the calculation is slightly different. The electrical exergy efficiency of the μ-CHP needs to be replaced, in this case, by the overall exergy efficiency of the μ-CHP system. The results are given in Table 10. In this table also an indication is given for the total number of μ-CHP units that can be fuelled by one single hydrogen plant based on the same amount biomass input. This value is calculated by

Table 9
Results for the three μ-CHP systems fuelled with two different fuels.

	PEM2		PEM3	
	Hydrogen1	Hydrogen2	Hydrogen1	Hydrogen2
Hydrogen purity [%]	60	99.99	60	99.99
Fuel input [g s^{-1}]	0.439	0.037	0.384	0.032
Air input [g s^{-1}]	2.639	2.530	1.834	1.782
Voltage fuel cell [V]	0.534	0.549	0.534	0.549
Fuel cell area [m^2]	0.273	0.265	0.320	0.309
Auxiliary power [W]	126.48	121.27	317.34	309.07
Electrical exergy efficiency [%]	22.09	23.04	25.27	26.26
Overall energy efficiency [%]	89.96	90.73	102.86	103.28
Overall exergy efficiency [%]	30.14	31.46	34.48	35.84

Table 10
Efficiencies for the whole chain.

	Hydrogen1 (60% pure H_2)		Hydrogen2 (99.99% pure H_2)	
	PEM2	PEM3	PEM2	PEM3
Electric energy efficiency of the chain [%]	15.51	17.74	13.64	15.53
Electric exergy efficiency of the chain [%]	13.57	15.52	11.67	13.29
Total energy efficiency of the chain [%]	62.02	70.90	54.54	62.09
Total exergy efficiency of the chain [%]	18.52	21.19	15.92	18.14
Number of units that could be fuelled	9233	10,031	7864	8558

dividing the output of the hydrogen plant by the fuel input of the μ-CHP.

5. Discussion

The calculated carbon dioxide fraction of the producer gas at the exit of the gasifier in the hydrogen production plants is 17 vol%. This is approximately 7 percentage points higher than was found in the literature [32]. As the composition of the biomass was not given in the literature, the difference may result from differences in the biomass. The exergy losses calculated for the hydrogen2 plant are larger than for hydrogen1, as indicated in Fig. 4. A large problem in the purification is the great loss of valuable hydrogen. In a PSA system some hydrogen is used to purge the adsorber; the used hydrogen is lost. This amount of hydrogen is larger than the amount of hydrogen assumed to be oxidized in the preferential oxidation process.

The purity of the hydrogen is an important factor when used in PEM fuel cells, since these fuel cells are very sensitive towards impurities, especially carbon monoxide. When using pure hydrogen little problems will arise due to impurities. When using less pure fuels like the 60% hydrogen problems seem to be inevitable. Although, the technology is still developing, especially the search for more tolerant electrodes is still ongoing. As well as the research towards improvements in the gas processing techniques, like preferential oxidation. It is likely that the developments in both technologies will meet somewhere midway, with a more tolerant fuel cell and a more effective preferential oxidation. For instance, it could be possible to attain similar performance of the fuel cell operating on 100 ppm CO/H_2 compared to a fuel cell operating on pure hydrogen, according to Kawatsu [48]. The nitrogen in the 60% hydrogen act only as a diluent in the PEM fuel cell systems [44]. Platinum is a good catalyst for methane oxidation [49]. However, the methane content is very low and the fuel cell temperature is also low, its effect on the PEM fuel cell performance is negligible.

The size of the fuel cell system as well as the hydrogen distribution grid is influenced by the quality of the fuel. In the case of 60% hydrogen more compression power and also larger pipe diameters are necessary than in the case of pure hydrogen, because of the higher volume per mole of hydrogen. Despite the higher compression cost and the lower μ-CHP efficiencies the chain efficiencies are higher for the systems fuelled with fuel from hydrogen1 (60% hydrogen). The lower efficiencies of systems with pure hydrogen are caused by the large losses during the purification process of hydrogen2. Also the number of μ-CHP units that can be fuelled by one hydrogen1 plant using the same biomass flow will be larger. This is caused by the large amount of hydrogen which is lost during the purification in hydrogen2.

There is a large difference in the mass flows for the two different hydrogen rich fuels to the μ-CHP system. This is caused by the impurities in the 60% hydrogen. The molecular weight of the impurities is much higher than the molecular weight of hydrogen. When looking at the volume flow, the difference is less. The volumetric flow of the 60% hydrogen is only 31% larger than the pure hydrogen to the μ-CHP system. This larger volume flow results also in an increased required compression power. The lower concentration of hydrogen in the 60% hydrogen results in a lower cell voltage.

The way additional heat is being produced has an influence on the efficiency of the μ-CHP system and on the energy conversion chain. The direct combustion of hydrogen for the production of additional heat leads to large exergy losses. The use of a heat pump can reduce these losses significantly. When the efficiency of the fuel cell increases, the efficiency difference between PEM2 and PEM3 will be larger. Further improvement of the electrical efficiency of the PEM fuel cell as well as the COP of the heat pump can significantly improve the performance of the whole chain.

The heat and electrical power demands of dwellings are strongly fluctuating. A μ-CHP system must be able to manage these fluctuations. High peaks in the heat demand are easier handled by a combustor than by a heat pump. Heat buffers can be helpful to supply the heat also during fluctuating demands. Variations in load are not considered in this study; the response of the system on different heat and power demands is beyond the scope of this work. This study is limited to the systems performance at full load. In actual systems the μ-CHP units will operate at part load for most of the time. This will influence the efficiencies of the μ-CHP systems. The PEM fuel cell unit can in principle have a higher conversion efficiency, because of the higher cell voltage at part load conditions.

6. Conclusions

The combination of centralized hydrogen production with decentralized power production with PEM fuel cells has been assessed by modelling the considered system alternatives in Cycle-Tempo. The hydrogen production is based on biomass gasification using a FICFB gasifier. PEM fuel cell units are used for the decentralized power production. Two hydrogen production plants have been modelled. The first one is called hydrogen1 and produces 60% hydrogen with an exergy efficiency of 61.3%. The second one is called hydrogen2, produces 99.99% pure hydrogen with an exergy efficiency of 50.6%. The hydrogen produced by these plants is assumed to be fed to a hydrogen distribution grid.

Decentralized power production is supposed to occur in μ-CHP units. Each unit generates 1 kW of electricity and 3 kW of heat. The μ-CHP units are connected to the hydrogen distribution grid. By comparing the units fuelled with 60% and 99.99% pure hydrogen, the effect of the purity of hydrogen on the performance of the μ-CHP units is evaluated.

Two different ways for the production of all demanded heat by the μ-CHP units are considered. Two alternative designs have been made, PEM2 and PEM3. In PEM2 a fuel by-pass to the boiler is added, so extra fuel can be combusted for heat production. For PEM3, a ground coupled heat pump is supposed to produce additional heat. The total exergy efficiencies (electricity and heat) for 60% hydrogen to the PEM2 and PEM3 units are respectively 30.3% and 32.9%. The values for 99.99% pure hydrogen are respectively 31.6% and 34.4%. The overall performance of the μ-CHP units fuelled with 60% hydrogen is lower than one fuelled with 99.99% pure hydrogen.

At the end the whole chain of hydrogen production towards the generation of heat and power has to be considered. The total exergy efficiency of this chain, with the PEM2 and 60% hydrogen is 18.4%. In case of 99.99% pure hydrogen the chain exergy efficiency is 15.9%. For PEM3, these values are respectively 19.9% and 17.3%. The use of impure hydrogen results in a better thermodynamic performance.

However, it results in larger dimensions (30%) of the equipment because of the higher volume flows of fuel per unit power.

If the whole chain is considered, the PEM3 system with 60% hydrogen gives the highest overall exergy efficiency.

Higher efficiencies of the PEM fuel cell as well as higher COP values of the heat pump will improve the overall exergy efficiency of the whole chain. The calculated exergy efficiencies of the considered conversion chains appear not to be very promising. A search for further improvement or alternative system options seems to be useful. For instance, the centralized conversion of biomass into fuel and the centralized conversion of that fuel into electricity, like is done in an earlier study [20].

References

[1] A.V. Bridgwater, Fuel 74 (1995) 631–653.
[2] T. Kivisaari, P. Bjornbom, C. Sylwan, J. Power Sources 104 (2002) 115–124.
[3] D.R. McIlveen-Wright, J.T. McMullan, D.J. Guiney, J. Power Sources 118 (2003) 393–404.
[4] K.D. Panopoulos, L.E. Fryda, J. Karl, S. Poulou, E. Kakaras, J. Power Sources 159 (2006) 570–585.
[5] G. Donolo, G.D. Simon, M. Fermeglia, J. Power Sources 158 (2006) 1282–1289.
[6] K.V. Lobachyov, H.J. Richter, Energy Convers. Manage. 39 (1998) 1931–1943.
[7] S. Cordiner, M. Feola, V. Mulone, F. Romanelli, Appl. Therm. Eng. 27 (2007) 738–747.
[8] S. Ghosh, S. De, Proc. Inst. Mech. Eng. A: J. Power Energy 217 (2003) 575–581.
[9] J.E. Hustad, H. Hofbauer, A. Vik, J. Byrknes, BioSOFC—technology development for integrated SOFC, biomass gasification and high temperature gas cleaning, in: Biomass Conference, Biomass for Energy, Industry and Climate Protection, Rome, 2004.
[10] C. Athanasiou, F. Coutelieris, E. Vakouftsi, V. Skoulou, E. Antonakou, G. Marnellos, A. Zabaniotou, Int. J. Hydrogen Energy 32 (2007) 337–342.
[11] A.O. Omosun, A. Bauen, N.P. Brandon, C.S. Adjiman, D. Hart, J. Power Sources 131 (2004) 96–106.
[12] N.C. Monanteras, C.A. Frangopoulos, Energy Convers. Manage. 40 (1999) 1733–1742.
[13] H. Morita, F. Yoshiba, N. Woudstra, K. Hemmes, H. Spliethoff, J. Power Sources 138 (2004) 31–40.
[14] S. Ghosh, S. De, Energy 31 (2006) 345–363.
[15] T. Seitarides, C. Athanasiou, A. Zabaniotou, Renew. Sustain. Energy Rev. 12 (2008) 1251–1276.
[16] T. Proell, C. Aichernig, R. Rauch, H. Hofbauer, Coupling of biomass steam gasification and an SOFC—gas turbine hybrid system for highly efficient electricity generation, in: ASME Turbo Expo 2004: Power for Land, Sea, and Air, Vienna, Austria, 2004.
[17] L. Fryda, K.D. Panopoulos, E. Kakaras, Energy Convers. Manage. 49 (2008) 281–290.
[18] L. Fryda, K.D. Panopoulos, J. Karl, E. Kakaras, Energy 33 (2008) 292–299.
[19] S. Karellas, J. Karl, E. Kakaras, Energy 33 (2008) 284–291.
[20] R. Toonssen, N. Woudstr, A.H.M. Verkooijen, Reference system for a power plant based on biomass gasification and SOFC, in: 8th European Solid Oxide Fuel Cell Forum, Luzerne, Switzerland, 2008.
[21] M. Sucipta, S. Kimijima, T.W. Song, K. Suzuki, J. Fuel Cell Sci. Technol. 5 (2008) 041006.
[22] P.V. Aravind, T. Woudstra, N. Woudstra, H. Spliethoff, J. Power Sources, doi:10.1016/j.jpowsour.2009.01.017.
[23] J. Karl, N. Frank, S. Karellas, M. Saule, U. Hohenwarter, J. Fuel Cell Sci. Technol. 6 (2009) 021005.
[24] A. Ersoz, S. Ozdogan, E. Caglayan, H. Olgun, J. Fuel Cell Sci. Technol. 3 (2006) 422–427.
[25] A. Sordi, E.P. Silva, L.F. Milanez, D.D. Lobkov, S.N.M. Souza, Braz. J. Chem. Eng. 26 (2009) 159–169.
[26] G. Gigliucci, L. Petruzzi, E. Cerelli, A. Garzisi, A. La Mendola, J. Power Sources 131 (2004) 62–68.
[27] M.H. Saidi, M.A. Ehyaei, A. Abbasi, J. Power Sources 143 (2005) 179–184.
[28] W.G. Colella, J. Power Sources 118 (2003) 118–128.
[29] S. Page, S. Krumdieck, Energy Policy, doi:10.1016/j.enpol.2008.11.009 (2009).
[30] M. Bolhar-Nordenkampf, K. Bosch, R. Rauch, S. Kaiser, H. Tremmel, C. Aichernig, H. Hofbauer, Scale-up of a 100 kWth pilot FICFB-gasifier to a 8 MWth FICFB-gasifier demonstration plant in Güssing (Austria), in: 1st International Ukrainian Conference on BIOMASS FOR ENERGY, Kiev, Ukraine, 2002.
[31] M. Bolhar-Nordenkampf, H. Hofbauer, Gasification demonstration plants in Austria, in: International Slovak Biomass Forum, Bratislava, 2004.
[32] H. Hofbauer, R. Rauch, G. Loeffler, S. Kaiser, E. Fercher, H. Tremmel, Six years experience with the FICFB-gasification process, in: 12th European Conference and Technology Exhibition on Biomass for Energy, Industry and Climate Protection, Amsterdam, The Netherlands, 2002.
[33] H. Hofbauer, R. Rauch, K. Bosch, R. Kock, C. Aichernig, Biomass CHP plant Güssing—a success story, in: Expert Meeting on Pyrolysis and Gasification of Biomass and Waste, Strasbourg, 2002.
[34] H. Hofbauer, R. Rauch, P. Foscolo, D. Matera, Hydrogen-rich gas from biomass steam gasification, in: 1st World Conference and Exhibition on Biomass for Energy and Industry, Sevilla, Spain, 2000.
[35] R. Toonssen, N. Woudstr, A.H.M. Verkooijen, Int. J Hydrogen Energy 33 (2008) 4074–4082.
[36] C.N. Hamelinck, A.P.C. Faaij, Future Prospects for Production of Methanol and Hydrogen from Biomass, Copernicus Institute, University Utrecht, 2001.
[37] P. McKendry, Bioresour. Technol. 83 (2002) 55–63.
[38] M.V. Twigg, Catalyst Handbook, Wolfe Publishing Ltd., London, 1989.
[39] A. Wootsch, C. Descorme, D. Duprez, J. Catal. 225 (2004) 259–266.
[40] J.M. Zalc, D.G. Löffler, J. Power Sources 111 (2002) 58–64.
[41] X. Cheng, Z. Shi, N. Glass, L. Zhang, J. Zhang, D. Song, Z.-S. Liu, H. Wang, J. Shen, J. Power Sources 165 (2007) 739–756.
[42] G.J.M. Janssen, J. Power Sources 136 (2004) 45–54.
[43] D.C. Papageorgopoulos, F.A. de Bruijn, J. Electrochem. Soc. 149 (2002) A140–A145.
[44] EG&G Techincal Services, Fuel Cell Handbook, Nation Energy Technology Laboratory, Morgantown, 2004.
[45] Cycle-Tempo, 5.0, TU Delft, 2006, www.cycle-tempo.nl.
[46] J. Szargut, D.R. Morris, F.R. Steward, Exergy Analysis of Thermal, Chemical, and Metallurgical Processes, Springer-Verlag, Berlin, 1988.
[47] S.H. Lee, J. Han, K.-Y. Lee, J. Power Sources 109 (2002) 394–402.
[48] S. Kawatsu, J. Power Sources 71 (1998) 150–155.
[49] R.A. Periana, D.J. Taube, S. Gamble, H. Taube, T. Satoh, H. Fujii, Science 280 (1998) 560–564.
[50] K.V. van der Nat, N.N. Woudstr, H. Spliethoff, Evaluation of several biomass gasification processes for the production of a hydrogen rich synthesis gas, in: International Hydrogen Energy Congress and Exhibition IHEC 2005, Istanbul, 2005.
[51] S.-H. Ge, B.-L. Yi, J. Power Sources 124 (2003) 1–11.